Quantum Electronics **46** (6) 567–573 (2016)

DOI: 10.1070/QEL15710

Model of a laser gyroscope with frequency dithering

V.K. Sakharov

Abstract. **The model of a laser gyroscope (LG) with frequency dithering is described by a system of recurrent equations for the electric fields of counterpropagating waves. The phenomenon of frequency locking is taken into account in the form of the wave coupling through backward scattering; the frequency bias factor is the controlled phase nonreciprocity. The character of the output signal is considered, which corresponds to two types of frequency dithering, namely, sinusoidal and in the form of meander that are produced by various methods, including intracavity phase modulation. Results of calculation of a frequency characteristic of the LG are presented as functions of frequency dithering, rotational velocity and LG parameters. It is shown that the method of processing an output signal by measuring the time interval between intensity oscillations has an advantage due to the absence of so-called dynamic lock-in zones in the output characteristic.**

Keywords: *laser gyroscope, lock-in, frequency dither.*

1. Introduction

It is known that a He–Ne gyroscope is the only type of a laser gyroscope (LG) with practical applications. The main reason of failures in the development of other LG types is the frequency lock-in (mutual synchronisation) of counterpropagating waves, which occurs due to backscattering of oncoming waves and is revealed in that the device does not react to small rotational velocities.

The frequency lock-in can be eliminated by the use of frequency dithering that is implemented as a phase (frequency) nonreciprocity introduced into a ring resonator. It results in that the frequencies of the counterpropagating waves differ by a considerable value such that the lock-in fails. In gaseous LG engineering, in most cases the frequency dithering is formed by mechanical dithering or by magneto-optical devices based on Faraday, Zeeman or Kerr effects [1–3].

Until quite recently, in semiconductor LGs that have a substantially lower sensitivity, the frequency dithering has not been used, because the level of backscattering in this case is higher by several orders of magnitude; hence, the width of the lock-in zone is greater, and it is very difficult or impossible to provide a frequency bias in these conditions.

The situation has changed with the conclusion made in [4] from the model of the frequency lock-in: in a semiconductor LG in the case of a long ring resonator formed by an optical fibre, the lock-in zone width reduces. Thus, it becomes evident that the frequency dithering can be used and there is a simple method for implementing it – intracavity phase modulation by a sinusoidal signal applied to a piezoelectric actuator [5].

The resulting sensitivity of a semiconductor LG has increased by at least three orders of magnitude as compared to similar devices described previously [6–9]. Thus, the possibility and promising employment of frequency dithering in investigations aimed at designing semiconductor (solid-state) LGs has been revealed. Thus, the model [4] needs improvement in order to be applicable to the case of frequency dithering that is formed by intracavity modulation.

In solving this problem, it seems reasonable to expand the scope of applications of this model to other types of LGs and methods of obtaining a frequency bias. In contrast to the known model based on the analogy between the phenomena of the frequency lock-in and interaction of two coupled oscillating circuits [10, 11], in the presented model the character and parameters of circulating radiation are determined by the factors which directly affect the counterpropagating waves. It was supposed that some new features of LG generation regimes might be revealed, which favour a better understanding of the physics of operation of such a device.

Thus, in the model suggested, the lock-in phenomenon is taken into account in the form of the wave coupling through backscattering; frequency dithering is considered as a result of a controlled action on wave amplitudes and phases in some way; the model is written in the form of a system of recurrent equations (in two variants) for complex amplitudes of the electric fields of the waves.

The method of forming an alternating-sign frequency bias in the form of sinus and meander by intracavity phase modulation is thoroughly discussed along with other methods (concise) well known and applied in practice. The intended application of the model is considered, namely, modelling of LG operation; it is shown that the character of beats at the output depends on the shape of frequency dithering, rotational velocity and LG parameters, including the length of the resonator, the level and random phases of the backscattering. The frequency characteristic has been calculated, which relates the beating frequency to these factors.

In the last part of the work, two methods for processing the output signal are considered: the first conventionally used in the technique of He–Ne gyroscopes, which employs a reverse count of the number of oscillations in neighbouring half-cycles of the bias; and the second based on measuring the time intervals between these oscillations. The advantage of the second approach is shown, i.e. the absence of 'dynamic lock-in zones' in the form of small flats in the output charac-

V.K. Sakharov JSC 'Center VOSPI', ul. Vvedenskogo 3, 117432 Moscow, Russia; e-mail: info@centervospi.ru

Received 6 November 2014, revised 22 September 2015
Kvantovaya Elektronika **46** (6) 567–573 (2016)
Translated by N.A. Raspopov

teristic which relates the measured rotational velocity to the real velocity. This indicates that the origin of flats is related to the method of processing the output signal.

2. Presuppositions

When counterpropagating waves run over a rotating closed optical loop (resonator) as a result of the Sagnac effect, the phase of one wave, let it be wave A, increases by a value δ_S, whereas the phase of the other wave, B, reduces by the same value. As a result, the phase difference of the waves, $2\delta_S$, arises, which, if we assume that this phase difference is regularly accumulated in the circulation process and the waves are presented by single-mode radiation, could lead to beats with the frequency

$$\nu_S = \frac{2\delta_S}{2\pi\tau} = M\Omega, \tag{1}$$

where $\tau = Ln/c$ is the time needed for the wave to run over the resonator loop; L is the resonator length; Ω is the rotational velocity; $M = 4S/(\lambda Ln)$ is the scaling coefficient; S is the area of the loop (if a fibre coil is used, S is determined by the product of the coil area by the number of turns of the fibre); λ is the radiation wavelength; and n is the refractive index of resonator medium. It is also assumed that the plane of the coil is normal to the axis of rotation.

However, in a real LG at a low rotational velocity the frequency is locked in, and hence there are no beats. Nevertheless, if the rotational velocity increases, beats arise and their frequency ν_{beat} coincides with the Sagnac beat frequency ν_S. At a higher rotational velocity and a lower level of backscattering, the coincidence is better.

The same character of LG emission is specific for model [4], where the backscattering is assumed concentrated at a single point inside a ring resonator. At this point, the counterpropagating waves circulating in the ring resonator are described by the recurrent equations

$$\begin{aligned} A_p &= A_{p-1}\exp(\mathrm{j}\delta_S) + \sqrt{\alpha}B_{p-1}\exp(-\mathrm{j}\delta_S), \\ B_p &= B_{p-1}\exp(-\mathrm{j}\delta_S) + \sqrt{\alpha}A_{p-1}\exp(\mathrm{j}\delta_S), \end{aligned} \tag{2}$$

where $A_p = a_p\exp(\mathrm{j}\phi_p)$ and $B_p = b_p\exp(\mathrm{j}\varphi_p)$ are the complex amplitudes of the electric fields of the waves; a_p, b_p and ϕ_p, φ_p are the moduli and phases of the waves, respectively; p is the circulation number counted from an arbitrarily chosen beginning; and α is the backscattering coefficient with respect to intensity.

In order to make this model applicable to an LG with frequency dithering, the former should be correspondingly improved. It is also important to remove the limitation concerning localisation of backscattering: now we will suppose that the backscattering is formed by a great number of scattering centres that are randomly located.

We assume that each of the counterpropagating waves is still single-mode radiation, the polarisation of scattered light is linear and coincides with that of the counterpropagating waves, the phase fluctuations arising due to spontaneous emission in the gain medium and the nonlinear effects in the ring resonator and active medium are neglected; finally, we do not take into account the concurrent wave competition assuming the two-wave generation regime to be stable. The latter assumption requires explanation.

It is known that in the case of a gaseous LG the competition of counterpropagating waves is excluded due to inhomogeneous broadening of the gain related to the Doppler mechanism of broadening and employment of a frequency bias. The possibility of stable bidirectional operation of a ring laser with homogeneously broadened gain (such a regime is realised at a sufficiently strong coupling between the counterpropagating waves through backscattering) was mentioned in [12]. This also follows from results of modelling by the considered model and from experiments: a stable bidirectional regime of generation was observed in [4–7, 9] devoted to the study of semiconductor LGs, in which, as mentioned, the level of backscattering is substantial. Finally, if in an LG of particular type the competition of counterpropagating waves is possible, there exist methods for suppressing it [8].

3. Model equations (first variant)

To take into account the phase (frequency) nonreciprocity of counterpropagating waves produced externally in some way, we substitute phases $\pm\delta_S$ in (2) for the phases

$$\Delta_A = \delta_S + \Phi_A(t), \quad \Delta_B = -\delta_S + \Phi_B(t), \tag{3}$$

where $\Phi_A(t)$ and $\Phi_B(t)$ are the phases related to the external action.

In a ring resonator, we choose point Q where a device is placed for extracting part of the power of counterpropagating waves. From this point we will count the coordinates of scattering centres x_i in the propagation direction of the wave, namely, B. Backscattered waves arising in scattering on each ith centre can be written in the form $A_i^{back} = \eta_i^A A_{p-1}$ and $B_i^{back} = \eta_i^B B_{p-1}$, where $\eta_i^{A,B} = \gamma_i\exp(\mathrm{j}\chi_i^{A,B})$ is a complex coefficient of backscattering. The backscattering is assumed isotropic; hence, the moduli of these coefficients for opposite propagation directions are equal, that is, $\gamma_i^A = \gamma_i^B$, and the imaginary parts are random values.

Then, at point Q the waves can be presented in the form

$$\begin{aligned} A_{i,p}^{back} &= \gamma_i A_{p-1}\exp[\mathrm{j}(\delta_S - 2kx_i + \chi_i^A) + \Phi_A(t)], \\ B_{i,p}^{back} &= \gamma_i B_{p-1}\exp[\mathrm{j}(-\delta_S + 2kx_i + \chi_i^B) + \Phi_B(t)], \end{aligned} \tag{4}$$

where the phases $\pm 2kx_i$ arise due to different distances of scattering centres from point Q; and $k = 2\pi n/\lambda$ is the wave number.

Finally, taking into account that the number of scattering centres is large and they are located chaotically in the ring resonator, the two backscattered waves that are sums of all backscattered waves in (4) from all scattering centres can be presented as follows:

$$\begin{aligned} A_{p-1}^{back} &= \sqrt{\alpha}\,A_{p-1}\exp[\mathrm{j}(\Delta_A + \tilde{\theta}_A)], \\ B_{p-1}^{back} &= \sqrt{\alpha}\,B_{p-1}\exp[\mathrm{j}(\Delta_B + \tilde{\theta}_B)], \end{aligned} \tag{5}$$

where $\alpha = \sum\gamma_i^2$ is the intensity of backscattered waves; and $\tilde{\theta}_A$ and $\tilde{\theta}_B$ are the random phases.

Thus, Eqns (2), which take into account the wave nonreciprocity and integral and random character of backscattering, take the form

$$\begin{aligned} A_p &= A_{p-1}\exp(\mathrm{j}\Delta_A) + \sqrt{\alpha}\,B_{p-1}\exp[\mathrm{j}(\Delta_B + \tilde{\theta}_B)], \\ B_p &= B_{p-1}\exp(\mathrm{j}\Delta_B) + \sqrt{\alpha}\,A_{p-1}\exp[\mathrm{j}(\Delta_A + \tilde{\theta}_A)]. \end{aligned} \tag{6}$$

Equations (6) give a mathematical presentation of the model of the considered LG with frequency dithering. One should pay attention to the constraint on the sum of intensities of counterpropagating waves that is actually realised in an amplifying medium,

$$|A_p|^2 + |B_p|^2 = \text{const}, \tag{7}$$

and to initial values of the complex amplitudes of counterpropagating waves.

From the calculations described below one can see that, depending on the rotational velocity, intensities and random phases of backscattering, resonator length and other parameters, either the beating or the lock-in regime is realised. In this case, the first summands in the right parts of (6) describe the accumulation of the phases of counterpropagating waves due to the frequency bias and to the Sagnac effect, which finally results in beats. The second summands are responsible for the mechanism of the frequency lock-in, which hinders phase accumulation and beats.

4. Intracavity phase modulation and the second variant of model equations

Consider the method of forming the frequency dithering by intracavity phase modulation and show in which way Eqns (6) can be presented in another form that can better reveal the role of frequency dithering in LG operation and will be used in calculations of the bias.

It is assumed that a phase modulator is placed at a random point of a ring resonator, the signal controlling the modulator is harmonic, and the modulator similarly affects the phases of counterpropagating waves, so that in passing across the modulator the waves acquire the same increment $\Phi(t) = \Phi_0 \sin(2\pi\nu_m t + \chi_0)$, where Φ_0, ν_m, and χ_0 are the amplitude, frequency and phase of modulation, respectively.

However, at every point Q of the ring resonator except for one point (in which the times τ_A and τ_B needed for the waves A and B to cover a distance from the phase modulator to point Q are equal) the phases of the waves after each successive circulation are different: $\Phi_A(t) = \Phi(t - \tau_A)$ and $\Phi_B(t) = \Phi(t - \tau_B)$, the sign of the phase difference $\Delta\Phi(t) = \Phi_A(t) - \Phi_B(t)$ being unchanged on time intervals equal to half the cycle of phase modulation.

From this follows that, similarly to the case where constant and small in value Sagnac phases $\pm\delta_S$ lead to beats, the relatively slow varying and slightly different modulation phases $\Phi_A(t)$ and $\Phi_B(t)$ also produce beats. This is confirmed by calculations according to (6).

From the calculation it also follows that the result will be the same, if each of the phases $\Phi_A(t)$ and $\Phi_B(t)$ changes; however, their difference $\Delta\Phi(t)$ is maintained constant. Then the phases $\Phi_A(t)$ and $\Phi_B(t)$ in (3) can be substituted for the phases $\Phi'_A(t) = \Delta\Phi(t)/2$ and $\Phi'_B(t) = -\Delta\Phi(t)/2$ and after introducing the frequency

$$\nu_d(t) = \frac{\Delta\Phi(t)}{2\pi\tau} = \frac{\Phi_A(t) - \Phi_B(t)}{2\pi\tau}, \tag{8}$$

we can rewrite (3) as follows

$$\Delta_A = \pi\tau\nu_S + \pi\tau\nu_d(t), \quad \Delta_B = -\pi\tau\nu_S + \pi\tau\nu_d(t); \tag{9}$$

note, that according to (8) the frequency $\nu_d(t)$ is determined by the phase difference $\Delta\Phi(t)$ in the same way as the beat frequency ν_S is determined by the difference of the Sagnac phases $2\delta_S$ according to (1).

Now, by substituting (9) into (6) we obtain another representation of the model equations:

$$\begin{aligned} A_p &= A_{p-1}\exp[j\pi\tau\nu(t)] + \sqrt{\alpha}\, B_{p-1}\exp[-j\pi\tau\nu(t) + \tilde{\theta}_B], \\ B_p &= B_{p-1}\exp[-j\pi\tau\nu(t)] + \sqrt{\alpha}\, A_{p-1}\exp[-j\pi\tau\nu(t) + \tilde{\theta}_A], \end{aligned} \tag{10}$$

where $\nu(t) = \nu_S + \nu_d(t)$, from which follows that the term $\nu_d(t)$ has a sense of frequency dithering.

5. Variants of alternating-sign frequency bias

From the form of Eqns (10) it follows that the dynamics of the complex amplitudes of counterpropagating waves is determined by the parameters and character of the frequency dithering $\nu_d(t)$ and is independent of the method of its formation. Another consequence is that in the frameworks of the model considered, the Sagnac frequency ν_S and the dithering frequency $\nu_d(t)$ are equivalent. Thus, similarly to the fact that beats only arise at a high rotational velocity, in the case of the frequency dithering the beats may occur only at sufficiently high values of the bias.

In the case of phase modulation by a harmonic signal $\Phi(t) = \Phi_0 \sin(2\pi\nu_m t - \chi_0)$, the frequency dithering, according to (8), looks also as a harmonic function:

$$\nu_d(t) = -\Phi_0\nu_m \frac{\Delta\tau}{\tau}\cos[2\pi\nu_m(t - \tau/2) + \chi_0], \tag{11}$$

where $\Delta\tau = \tau_A - \tau_B$, and $\Delta\tau/\tau$ may be termed the geometrical factor that takes the maximal value of unity when point Q is located near the phase modulator.

Seemingly, the same mechanism is realised when the modulating signal has the form of an isosceles triangle, i.e., the phase difference $\Delta\Phi(t)$ of counterpropagating waves $\Phi_A(t)$ and $\Phi_B(t)$ at any point (except for the single point where $\tau_A = \tau_B$) periodically varies; it should be sufficient to initiate beats. For the modulation signal in the form $\Phi(t) = (2\Phi_0/\pi)\arcsin[\sin(2\pi\nu_m t) + \chi_0]$ the dithering frequency $\nu_d(t)$ has the form of meander, that is, periodically changing the sign it remains unchanged in the absolute value:

$$\nu_d(t) = \frac{\Delta\tau}{\tau}\,\frac{2\Phi_0\nu_m}{\pi}.$$

In He–Ne gyroscopes a sinusoidal bias is formed by torsional vibrations of the resonator (torsion suspension), and for producing dithering in the form of meander one can use the reverse rotation at a constant rotational velocity. The phase nonreciprocity in both the cases is a result of the Sagnac effect.

Based on the Faraday, Zeeman and Kerr magneto-optical effects, due to their low persistence, one can realise the frequency dithering of both types – in the form of sinus and meander [3]. Also, an obvious method of producing the frequency dithering is unidirectional rotation at a constant rotational velocity, which produces the dithering having a constant frequency $\nu_d = \text{const}$. This method is used in practice [13], but quite rarely because of the difficulties of providing a highly stable rotational velocity of the LG.

6. Character of beats at the LG output

In modelling LG operation, the main attention was paid to investigation of the character of beats and the dynamics of the phases of counterpropagating waves, because these factors determine the properties of the LG as a sensor of rotation. However, the modelling gives also a chance to study the dynamics of counterpropagating waves and to get convinced that one of the simplifying conditions formulated at the beginning of the work and concerning the wave competition is satisfied.

At a comparatively strong backscattering, the amplitudes of counterpropagating waves a_p and b_p that initially differ, rather quickly become equal and then do not change. Only in the case of the weakest (above 100 dB) backscattering, the effect of amplitude equalising vanishes. This result confirms the possibility of stable operation of a semiconductor LG in which the level of backscattering is below 50 dB; the case of weak backscattering refers to a He–Ne gyroscope where the inhomogeneously broadened gain and the frequency dithering remove the problem of wave competition.

As expected, at a finite level of backscattering in the case without frequency dithering, and at low rotational velocity, beats are absent and the lock-in regime is implemented. However, beats arise if there is frequency dithering or the rotational velocity is high. By considering beats as oscillations of the intensities of beat waves $I_{\text{beat}}(p)$ we will calculate them by using a conventional expression for the output signal of an interferometer:

$$I_{\text{beat}}(p) = 0.5[1 + \cos(\Delta\psi_p)], \tag{12}$$

where $\Delta\psi_p = \phi_p - \varphi_p$ is the phase difference of counterpropagating waves and, instead of the number of circulations p, one can use time t because these variables are related by the formula $t = p\tau$.

Without rotation, that is, at $\delta_S = 0$, the numbers of intensity oscillations in the time intervals corresponding to neighbouring half-cycles of the frequency dithering are always equal. If $\delta_S \neq 0$, that is, the ring laser rotates, the number and the frequencies of oscillations in neighbouring half-cycles of the dithering are different. At a positive value of the phase δ_S, the number and frequency of oscillations are greater in the half-cycle with the positive sign of the frequency dithering $\nu_d(t)$, than with negative. At the negative sign of the phase δ_S, that is, at the opposite direction of rotation, the number of oscillations is greater in the half-cycle with the negative sign of the dithering.

An example of beats in cases of the two variants of an alternating-sign frequency dithering, namely, sinusoidal and meander, is shown in Fig. 1. With the intracavity phase modulation, such dithering, as was shown in the previous section, is produced by phase modulating signals having the form of a sinusoid and meander. The following parameters of a semiconductor LG were used in the calculation: R = 5 cm, λ = 1.55 μm, L = 600 m, α = 40 dB, $\Delta\tau/\tau$ = 1, ν_m = 1.2 kHz and Φ_0 = 25 rad. The phase δ_S = 0.034 rad (Ω = 0.5 deg s^{-1}) was intentionally taken large in order to visually demonstrate the different character of oscillations in a motionless and rotating ring laser.

One can see that in the case of a meander bias, oscillations are located regularly in both half-cycles of the dithering, and their frequencies within each of the half-cycles are the same – in our example 13.6 and 24.5 kHz. With a sinusoidal bias, the beat frequency in the central part of half-cycles is approximately 23 and 34 kHz; however, towards the end of a half-cycle the frequency noticeably falls. Moreover, at the boundaries between the half-cycles, beats are absent and, obviously, the frequency lock-in dominates.

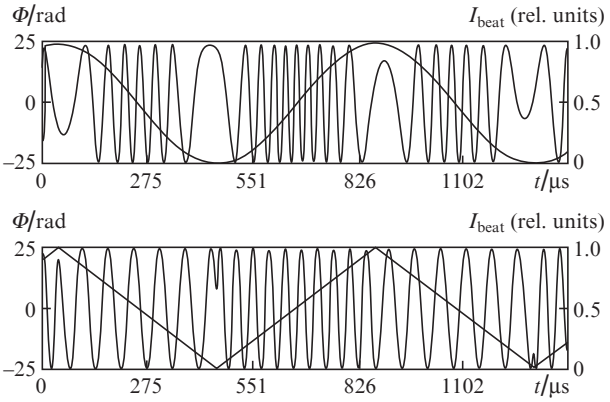

Figure 1. Phase modulation signals of sinusoidal and triangular shapes (ν_m = 1.2 kHz, Φ_0 = 25 rad) and beats at output of a semiconductor LG under the rotation at the velocity of Ω = 0.5 deg s^{-1}.

The same character of the output signal (equal and unequal numbers of oscillations in neighbouring half-cycles at rest and under rotation) is observed in modelling the operation of a He–Ne gyroscope. Naturally, in this case, other values of the resonator length and backscattering coefficient are specified, R = 20–50 cm and α = 80–120 dB, and other methods of simulating the dithering are employed, namely, by using a torsion suspension or a reverse rotation.

7. Frequency characteristic

A frequency characteristic relates the beat frequency of output waves ν_{beat} to a rotational velocity of the ring laser, LG parameters and the frequency dithering. A compact presentation of a frequency characteristic in the form of the function $\nu_{\text{beat}} = F(\nu, \alpha, L, \tilde{\theta}_A, \tilde{\theta}_B)$ is calculated from (10), where the time-dependent frequency $\nu(t)$ is substituted for a constant frequency ν, which can take arbitrary values and be the Sagnac frequency ν_S, the frequency ν_d (the dithering with a constant frequency ν_d = const=const), or the sum of these two frequencies.

A calculation of the frequency characteristics $\nu_{\text{beat}} = F(\nu, \alpha, L, \tilde{\theta}_A, \tilde{\theta}_B)$ includes specifying a series of values $\{\nu_i\}$, which cover a wide range of frequencies, calculation of the corresponding phase differences for two waves $\{\Delta\psi_p^i\}$ under the assumption of a sufficiently large value of p, and, finally, finding the frequency values ν_{beat}^i from the relationship

$$\nu_{\text{beat}}^i = \Delta\Psi_p^i/(2\pi p\tau). \tag{13}$$

Since the frequency characteristic is an odd function of frequency ν, the result of calculation, obtained as several frequency characteristics differing in some parameters, is presented graphically only for positive values of frequency ν (Fig. 2).

In Fig. 2, three groups of frequency characteristics for a semiconductor LG with a finite coefficient of backscattering are presented, and one characteristic, which corresponds to absolutely absent backscattering (the case of an ideal LG). For all characteristics R = 5 cm and λ = 1.55 μm, each group comprises the characteristics for a fixed resonator length (3 or

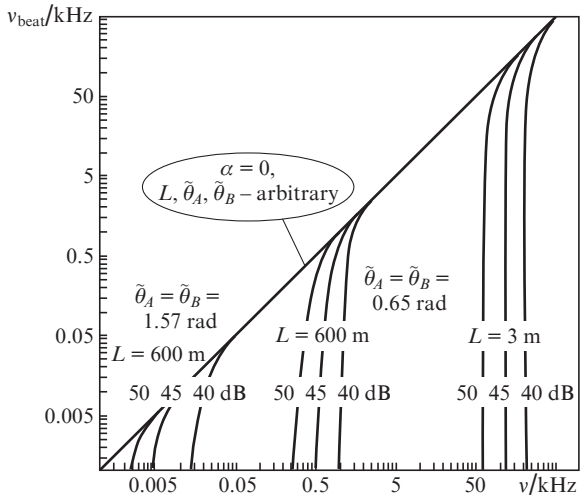

Figure 2. Frequency characteristics of a semiconductor LG $\nu_{beat} = F(\nu, \alpha, \tilde{\theta}_A, \tilde{\theta}_B)$.

600 m) and for three values of the backscattering coefficient α (40, 45, and 50 dB).

One can see that the beat frequency ν_{beat} in a low-frequency range for all characteristics except for the one, related to the ideal LG, takes a zero value, which points to the frequency lock-in in that range. It is a fundamental property: the frequency lock-in occurs in an LG even at a minimal backscattering level. The greater the backscattering, the wider the lock-in zone.

It is also seen that the width of the lock-in zone ν_{lock} also called the static lock-in zone depends on the length of the ring resonator. Thus, for a group of characteristics calculated at $L = 3$ m (it is an approximate length of ring resonators in semiconductor LGs in [6–8]), the width of the lock-in zones is 250–350 kHz, and at $L = 600$ m (the central group of characteristics) it is from 0.3 to 1.1 kHz. Recall that this important feature in the case of a long fibre in a semiconductor LG allows one to reduce the width of the lock-in zone and employ frequency dithering.

This effect is explained by that the level of backscattering in a semiconductor material is much higher than in a fibre. Hence, extension of the resonator length L does not result in an increase in α, which is determined by a sum of backscattered waves from all scattering centres in a circular optical tract. As a result, the effect of the frequency lock-in after each successive circulation remains unchanged; however, at increasing L, the number of circulations in a finite time interval reduces. In this way, the total result of the frequency lock-in reduces.

Frequency characteristics in Fig. 2 also show that as the frequency ν increases, the beat frequency ν_{beat}, after leaving the lock-in zone, rapidly rises and approaches a linear part of the characteristic. Thus, if the frequency ν is so high that the beat frequency ν_{beat} is 3–5 times greater than the width of the lock-in zone ν_{lock}, the LG reliably emerges from the lock-in regime. Moreover, in this case the beat frequency the most of time or all the time (the dithering in the form of sinus or meander, respectively) remains within the linear part of the frequency characteristic; hence, the beat frequency in these periods is determined by the expression

$$\nu_{beat} \cong \nu. \qquad (14)$$

Finally, let us consider the dependence of frequency characteristics on random phases $\tilde{\theta}_A$ and $\tilde{\theta}_B$. As was found, on the great part of the range of values of random phases, for example, in a square with a side width multiple of 2π, the width of lock-in zones ν_{lock} negligibly differs from the average value $\bar{\nu}_{lock}$ obtained by averaging ν_{lock} over the whole range. In this case, the widths of the lock-in zones at the phases satisfying the condition $\tilde{\theta}_A = \tilde{\theta}_B = 0.65$ rad coincide with the value $\bar{\nu}_{lock}$; this is why the most of frequency characteristics given in Fig. 2 have been calculated at these values of random phases.

The maximal width of the lock-in zone is above $\bar{\nu}_{lock}$ by at most 40%, and the minimal width may be substantially less. In Fig. 2, one can see that for the left group of frequency characteristics at the resonator length of 600 m and $\tilde{\theta}_A + \tilde{\theta}_B = \pm 2\pi$, the width of the lock-in zones is 3–11 Hz. However, extreme values only occur in small ranges of random phases, and the reason of the sharp fall of zone widths is a large value of phases $\tilde{\theta}_A$ and $\tilde{\theta}_B$, which substantially exceeds the phases Δ_A and Δ_B in (6); this results in a more rapid growth of the phase difference for counterpropagating waves $\Delta\psi_p$.

Such a dependence of frequency characteristics on random phases is observed, as was verified, for He–Ne gyroscopes as well.

8. Output signal processing by counting the number of oscillations

As known, a measurement of the angular rotational velocity or Sagnac frequency ν_S (1) by He–Ne gyroscopes is performed by converting intensity oscillations to a series of pulses which are then calculated and separately summed in even and odd half-cycles of the bias. The sought frequency ν_S (denote it ν_S^{out}) is calculated from the relationship $\nu_S^{out} = \Delta N/T$, where ΔN is the difference between the numbers of pulses in two half-cycles accumulated in a time interval $T \gg 1/\nu_m$.

In this case, the flats mentioned above arise on the output characteristic that gives a dependence of experimentally measured values of the angular rotational velocity Ω^{out} or frequency ν_S^{out} on real values. This is especially noticeable if torsion suspension is used; in the case of meander, this effect is less pronounced.

With the model considered, the output characteristics in both the cases are easily calculated. In the calculations, first the angular rotational velocity Ω or frequency ν_S is specified, then from (6) an array of phase differences $\{\Delta\psi_p\}$ is determined for two waves; a value of p is chosen corresponding to an integer number of frequency dithering periods K, that is, $p = K/(\tau\nu_m)$; the frequency ν_S^{out} is found (by the formula $\nu_S^{out} = \Delta\psi_p/(2\pi p\tau)$) and the angular rotational velocity Ω^{out}. In the course of calculations, the prescribed values Ω or ν_S are varied and in this way the output characteristic $\nu_S^{out} = F_{counts}(\nu_S)$ or $\Omega^{out} = F'_{counts}(\Omega)$ is obtained.

In Fig. 3, the characteristic $\nu_S^{out} = F_{counts}(\nu_S)$ obtained for a He–Ne gyroscope with a square resonator and the perimeter of 50 cm is presented. The method of torsion suspension was simulated with the bias amplitude of 32 kHz at the modulation (vibration) frequency of $\nu_m = 1.2$ kHz; Also, the coefficient $\alpha = 100$ dB and random phases $\tilde{\theta}_A = \tilde{\theta}_B = 0.65$ rad have been specified. One can see that the flats are located at the frequencies multiple of the frequency ν_m. The calculation yields that the width is greater at a higher backscattering coefficient; in addition, it depends on the modulation amplitude and frequency. In simulating the reverse rotation, flats also arise on

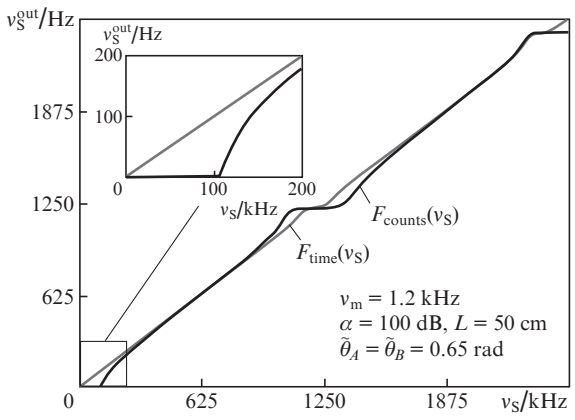

Figure 3. Output characteristics $\nu_S^{out} = F_{counts}(\nu_S)$ and $\nu_S^{out} = F_{time}(\nu_S)$ of the He–Ne gyroscope with vibration-reducing suspension.

the output characteristic, however, with a substantially smaller width.

The same behaviour of the output characteristics (with flats and the dependence on the type of bias) follows from a calculation of the output characteristic for a semiconductor LG with the dithering produced by intracavity phase modulation.

The reason of arising flats is, obviously, the frequency lock-in that occurs in short time intervals when the bias changes the sign. To eliminate flats one has to employ additional noise realised by mixing a small pseudo-random signal to the frequency dithering [14]. The measurement accuracy in this case increases, but due to the employment of the signal filtering that is necessary in this case, the duration of measurements becomes longer.

9. Output signal processing by measuring time between oscillations

The method of processing the output signal considered in this section eliminates origin of flats on the output characteristic. The approach was used in [5] for real-time processing of the output signal, and its functionality has been approved. However, the method needs a more thorough investigation with the numerical simulation of the corresponding algorithm of signal processing.

The method is based on the linear character of the frequency characteristic $\nu_{beat} = F(\nu, \alpha, L, \tilde{\theta}_A, \tilde{\theta}_B)$ which follows from (14) at a sufficiently high beat frequency; thus, the beat frequency can be presented in the form:

$$\nu_{beat}(t) \cong \nu_S + \nu_d(t). \tag{15}$$

Let us isolate in two neighbouring half-cycles of an alternating-sign frequency bias the pairs of oscillations separated by equal numbers q of the half-cycles and denote the maximal intensities $I_{beat}(p)$ on time scale in the pairs by t_1^+, t_2^+ and t_1^-, t_2^-. The phase difference for two waves, which corresponds to each pair of times, in one half-cycle will be $2\pi q$ and in the other half-cycle it will be $-2\pi q$, which can be written as follows

$$2\pi \int_{t_1^\pm}^{t_2^\pm} [\nu_S + \nu_d(t)]\,dt = \pm 2\pi q. \tag{16}$$

By combining two expressions (16) we obtain

$$\nu_S = \frac{1}{\Delta t^+ + \Delta t^-}\left(\int_{t_1^+}^{t_2^+} \nu_d(t)\,dt + \int_{t_1^-}^{t_2^-} \nu_d(t)\,dt\right), \tag{17}$$

where $\Delta t^+ = t_2^+ - t_1^+$.

In the case of the dithering in the form of meander, expression (17) is simplified

$$\nu_S = \frac{\Delta t^+ - \Delta t^-}{\Delta t^+ + \Delta t^-}|\nu_d|. \tag{18}$$

From (17) and (18) follows that, if the parameters of the frequency dithering are known, from detected beats $I_{beat}(t)$ one can find the frequency ν_S and, correspondingly, the rotational velocity Ω.

The method of processing beats under consideration was verified in two stages: at the first stage, the frequency ν_S was chosen, and LG operation was modelled in order to calculate the output signal; at the second stage, by modelling the algorithm described above, actually an inverse problem was solved, i.e., calculation of the frequency ν_S^{out}. In beat processing, operations that simulate the digital-to-analogue conversion of the output signal $I_{beat}(p)$ and formation of the corresponding sampling array have been employed. The sampling array was used for determining the times t_1^+, t_2^+ and t_1^-, t_2^-. A 'noise' signal in the form of chaotic pulses can be added to beats, in which case averaging procedures were used at various stages. Variation of the frequency ν_S in the calculations yielded the output characteristic $\nu_S^{out} = F_{time}(\nu_S)$.

An example of the output characteristic $\nu_S^{out} = F_{time}(\nu_S)$ calculated for a He–Ne gyroscope with torsion suspension and the parameters used in the previous sections is presented in Fig. 3. As one can see there are no flats and the characteristic looks like a straight line, which indicates that the specified and calculated frequencies coincide (within the error of at most 0.5%) $\nu_S^{out} \cong \nu_S$ over the whole range 0–2500 Hz. The dependence on the level of backscattering was noticeable only at a considerable backscattering for $\alpha < 20$ dB. A similar calculation for a semiconductor LG with phase modulation yields $\nu_S^{out} = F_{time}(\nu_S)$, which is also a straight line.

Thus, the modelling shows that the origin of flats is related to the method used for processing the output signal. The question whether this method is appropriate in the case of a He–Ne gyroscope requires a particular study.

10. Conclusions

The model of an LG with frequency dithering is suggested, which is described by a system of recurrent equations for the electric field of counterpropagating waves and is an alternative to the known model based on the analogy between the phenomena of the frequency lock-in and interaction of two coupled oscillating circuits.

In the frameworks of this model, the alternate-sign frequency bias is considered, which is produced in various ways, including intracavity phase modulation. It is shown, that the character of the output signal corresponds to two main types of dithering, i.e., sinusoidal and in the form of meander. The model is used for calculating the frequency characteristic as a function of the dithering frequency, the rotational velocity of a ring resonator and the LG parameters, which include the length of the ring resonator, the coefficients and random phases of backscattering.

In addition, two methods of output signal processing are considered and compared: by calculating the number of

intensity oscillations in neighbouring half-cycles of the frequency dithering and by measuring the time intervals between these oscillations. The demonstrated advantage of the second method is that there are no dynamic lock-in zones on the output characteristic, which are inherent in the first method and complicate its employment.

Acknowledgements. The author is grateful to L.P. Prokof'eva and V.V. Shcherbakov for their attention to the work.

References

1. Aronovits F. In: *Primenenie lazerov* (Application of Lasers) (Moscow: Mir, 1971).
2. Kuryatov V.N., Landa P.S., Lariontsev E.G. *Izv. Vyssh. Uchebn. Zaved., Ser. Radiofiz.*, **11**, 1839 (1968).
3. Azarova V.V., Golyaev Yu.D., Dmitriev V.G. *Kvantovaya Elektron.*, **30** (2), 96 (2000) [*Quantum Electron.*, **30**, 96 (2000)].
4. Sakharov V.K. *Zh. Tekh. Fiz.*, **81** (8), 76 (2011).
5. Prokof'eva L.P., Sakharov V.K., Shcherbakov V.V. *Kvantovaya Elektron.*, **44** (4), 362 (2014) [*Quantum Electron.*, **44**, 362 (2014)].
6. Taguchi K., Fukushima K., Ishitani A., Ikeda M. *Measurement*, **27**, 251 (2000).
7. Inagaki K., Tamura S., Noto H., Harayama T. *Phys. Rev. A*, **78**, 053822 (2008).
8. Mignot A., Feugnet G., Schwartz S., et al. *Opt. Lett.*, **34**, 9 (2009).
9. Akparov V.V., Dmitriev V.G., Duraev V.P., et al. *Kvantovaya Elektron.*, **40** (10), 851 (2010) [*Quantum Electron.*, **40**, 851 (2010)].
10. Adler R. *Proc. IRE*, №34, 352 (1946).
11. Klimontovich Yu.L. (Ed.) *Volnovye i fluktuatsionnye protsessy v lazerakh* (Wave and Fluctuation Processes in Lasers) (Moscow: Nauka, 1974).
12. Kravtsov N.V., Lariontsev E.G. *Kvantovaya Elektron.*, **21** (10), 903 (1994) [*Quantum Electron.*, **24**, 841 (1994)].
13. Wang B., Zhang W., Wang Z., Zhu P. *Mathematical Problems in Engineering* (Hindawi Publishing Corporation, 2013) Article ID 856803.
14. Khoshev I.M. *Kvantovaya Elektron.*, **7** (5), 953 (1980) [*Sov. J. Quantum Electron.*, **10**, 544 (1980)].